Differential effects of Mxi1-SRalpha and Mxi1-SRbeta in Myc antagonism.

Claire Dugast-Darzacq, Thierry Grange, Nicole B. Schreiber-Agus

Ce manuscrit a été publié dans FEBS Journal 274:4643-4653 (2007)

Differential effects of Mxi1-SRα and Mxi1-SRβ in Myc antagonism

Dugast-Darzacq Claire [1,2,*], **Grange Thierry [2]** and Schreiber-Agus Nicole B [1]

[1] Department of Molecular Genetics

Albert Einstein College of Medicine

Bronx, NY 10461 USA

[2] Institut Jacques Monod

CNRS-Universités de PARIS 6 et 7

75251 Paris cedex 05 – FRANCE

* Address correspondence to:

Claire Dugast-Darzacq, Ph.D.

Institut Jacques Monod

CNRS-Universités de PARIS 6 et 7

75251 Paris cedex 05 – FRANCE

darzacq@ijm.jussieu.fr

Phone : 33-1-44275707

Fax : 33-1-44275716

Running Title: Distinct functions of Mxi1 protein isoforms

Key words : Mxi1, Myc, isoforms, REF assay, transcription, GAPDH

Abstract

Mxi1 belongs to the Myc-Max-Mad transcription factor network. Two Mxi1 protein isoforms, Mxi1-SRα and Mxi1-SRβ, have been described recently to share many biological properties. Here we assign differential functions to these isoforms with respect to two distinct levels of Myc antagonism. Unlike Mxi1-SRβ, Mxi1-SRα is not a potent suppressor of the cellular transformation activity of Myc. Furthermore, while Mxi1-SRβ exhibits a repressive effect on the *MYC* promoter in transient expression assays, Mxi1-SRα activates this promoter. A specific domain of Mxi1-SRα contributes to these differences. Moreover GAPDH interacts with Mxi1-SRα and enhances its ability to activate the Myc promoter. Our findings suggest that *mxi1* gains functional complexity by encoding isoforms with shared and distinct activities.

Introduction

Members of the Myc oncoprotein family function as transcription factors that control various aspects of cellular behavior including cell growth, proliferation, differentiation, apoptosis, genomic stability, and tumorigenesis (reviewed recently in [1-4]). Deregulation of Myc contributes to the pathogenesis of a large proportion of human cancers (reviewed in [5,6]). This deregulation has been shown to occur at multiple levels including those that affect *myc* gene expression, Myc protein stability, and Myc biological activity. Normal regulation of Myc activity occurs by mechanisms that influence the Myc protein *per se* (for examples see [7]), and also through the functions of related members of the extended Myc-Max-Mad protein network (reviewed recently in [8]; note that the Mad subfamily recently has been renamed the Mxd subfamily).

The Mxi1 (a.k.a. Mxd2) protein first was described as a member of the Myc/Mad/Max network by virtue of its having a basic helix-loop-helix leucine zipper (bHLH/LZ) region similar to that of Myc and of its interaction with the obligate Myc DNA binding partner, Max [9]. In early models that defined Mxi1's function within this network, Mxi1 (as well as the related Mad family proteins) was proposed to be a Myc antagonist. This was based upon its ability to bind competitively with Myc both to the Max protein and, once complexed with Max, to shared DNA sequence motifs (E-boxes; CANNTG). Beyond this, it was realized that whereas Myc could transactivate gene expression at the E-box through the recruitment of various co-activators (see [2] and references therein), Mxi1 could repress gene expression there through its interaction with Sin3/HDAC (histone deacetylase) complexes ([10,11] and reviewed in [8]). The antagonism by Mxi1 on the molecular level correlated well with its ability to be a potent suppressor of Myc transformation activity in the rat embryo fibroblast (REF) assay, a surrogate assay for neoplastic transformation [10]. Interestingly, a

naturally occurring mouse Mxi1 protein isoform lacking the Sin3 recruitment domain (a.k.a. the SID), called Mxi1-WR, was unable to potently suppress Myc cotransformation activity in the REF assay [10]. This suggested that Myc antagonism and growth suppression was linked to the presence of a SID and its ability to recruit co-repressors.

Recently, our group and others have recognized that in addition to the Mxi1-WR isoform, other Mxi1 protein isoforms exist both in mouse and man [12-14]. Many of these isoforms appear to arise from alternative exon 1 (and promoter) usage within the *mxi1* genomic locus. One new isoform that we have described, Mxi1-SRα, exhibits many of the biological properties attributed originally to Mxi1 and outlined above (we have renamed the original Mxi1 isoform Mxi1-SRβ) [12]. Specifically, Mxi1-SRα can also bind to Max and to Sin3, and can function as a transcriptional repressor upon various reporter plasmids including synthetic E-box reporters. With respect to expression profiles, Mxi1-SRα and Mxi1-SRβ transcripts can be found together in the majority of newborn and adult mouse tissues examined on the gross level. However, tissue-specific expression patterns were also observed, including that Mxi1-SRα appears to be the predominant transcript in the adult intestine and in the developing embryo, while Mxi1-SRβ transcripts predominate in the adult liver and kidney [12].

In our initial description of Mxi1-SRα and its comparison to Mxi1-SRβ [12], we speculated that despite their apparent functional overlap in the assays employed in that study, the possibility existed for distinct functions for these two isoforms. In the present study, we have compared further the Mxi1-SRα and Mxi1-SRβ isoforms at the levels of Myc antagonism in the REF assay, subcellular localization, and transcriptional activity. Some of these analyses have assigned differential functions to the two isoforms, and we show that the unique amino terminal extension on Mxi1-SRα contributes to these differences. A possible basis for these differences may lie in the ability of Mxi1-SRα (but not of Mxi1-SRβ) to

recruit specific protein partners such as the nuclear GAPDH protein.

Results

Mxi1-SRα lacks the strong suppressive activity of Mxi1-SRβ in the REF assay

In our earlier report describing Mxi1-SRα, this isoform appeared functionally homologous to Mxi1-SRβ in that both could bind to Max and Sin3 and repress both basal and Myc- activated transcription of various reporter plasmids [12]. Based on these properties, we predicted that Mxi1-SRα would act like its Mxi1-SRβ counterpart to suppress Myc+Ras cotransformation activity in the REF assay. Expression constructs were generated encoding Myc-tagged versions of these two isoforms, as well as of the Mxi1-WR isoform that lacks the SID, and shown to give rise to proteins of the expected size expressed at similar levels (Fig. 1A). Each of these constructs (or empty vector) was introduced along with Myc and Ras into primary REFs, and the extent of foci formation was assessed ~10 days post-transfection. As shown in Figure 1B, the addition of Mxi1-SRβ to Myc+Ras transfections resulted in the expected 5-fold reduction in foci number relative to that obtained in the Myc+Ras+empty vector point (compare Fig. 1B black "SRβ" bar to Fig. 1B open "empty" bar; see also [10]). Surprisingly, the addition of Mxi1-SRα to Myc+Ras transfections resulted in at best a 2-fold reduction in foci number relative to the Myc+Ras+empty vector point (compare Fig. 1B grey "SRα" bar to Fig. 1B open "empty" bar). Indeed, Mxi1-SRα behaved comparably to Mxi1-WR in these assays (compare Fig. 1B grey "SRα" bar to Fig. 1B dotted "WR" bar). This was unexpected given that (i) the inability of Mxi1-WR to potently suppress Myc co-transformation has been attributed to its lack of a SID [10] and (ii) Mxi1-SRα harbors a Sin3-interacting SID that is ~70% homologous to the SID of Mxi1-SRβ [12].

We considered the possibility that the difference in suppression potential between

introduced Mxi1-SRα and Mxi1-SRβ could relate to disparities in their expression levels at the onset of foci formation. As such, we generated several expression constructs for Mxi1-SRα containing different lengths of 5'UTR, and tested these in *in vitro* transcription/translation assays followed by Western blotting, and in the REF assay (data not shown). Many of these constructs produced levels of Mxi1-SRα protein comparable to or greater than those of Mxi1-SRβ, yet they could still not potently suppress in the REF assay. To address this in another way, we tested whether the introduction of lower amounts of Mxi1-SRβ would compromise its suppression potential. Introduction of one-fifth the usual amount of Mxi1-SRβ to Myc+Ras transfections resulted in the same 5-fold reduction in foci formation observed with the usual dose of Mxi1-SRβ (compare Fig. 1B black "SRβ low" bar to Fig. 1B black "SRβ" bar). Together, these findings suggested that the differential effects of Mxi1-SRα and Mxi1-SRβ in the REF assay likely relate to variables aside from expression levels.

As another gauge of suppression potential, we examined the introduced Mxi1 isoforms in stable transformed cell lines established from foci that had emerged in the various transfection points of the REF assay (Fig. 1C). Transformed cell lines established from the Myc+Ras+Mxi1-SRα points consistently expressed detectable levels of introduced Mxi1-SRα as assessed by Western blotting analysis (Fig. 1C, arrowed ~52 kDa band in lanes α1 and α2 in comparison to corresponding area in lane E1 which is from cell lines established from the Myc+Ras+empty vector point). Once again, this finding of expressed exogenous Mxi1-SRα resembled what is seen with the SID-less Mxi1-WR isoform as we have reported previously [10]. In contrast, transformed cell lines established from the Myc+Ras+Mxi1-SRβ points failed to express detectable levels of introduced Mxi1-SRβ (Fig. 1C, lanes β1 and β2; and see also [10]). These results suggest that strong selective pressure against the expression of introduced Mxi1-SRβ, but not of Mxi1-SRα (or Mxi1-WR), exists during the

course of cellular transformation induced by Myc.

Mxi1-SRα appears to be localized to the nucleus like Mxi1-SRβ

The findings of the REF assay suggested that Mxi1-SRα and Mxi1-SRβ may encode differential functions with respect to their ability to antagonize Myc function. As a first attempt to uncover the molecular basis for this difference, we performed immunofluorescence assays on three different cell types after transfection with Myc or FLAG-tagged versions of Mxi1-SRα or Mxi1-SRβ (Fig. 2A). As shown in Figure 2B, Myc-tagged Mxi1-SRα and Myc-tagged Mxi1-SRβ each exhibit speckled nuclear staining in transfected U20S cells. Similar results were obtained after transfection of U20S cells with the Flag-tagged isoforms, as well as after transfection of any of these constructs into COS7 or NIH3T3 cells (Fig. 2C and data not shown). It should be noted that this Mxi1-SRα subcellular localization is not in complete agreement with a previous report from another group [13] which described a primarily cytoplasmic localization, with some nuclear staining as well. However, Mxi1-SRα is predicted to be nuclear by programs such as PSORT II (reliability 94.1% by the [15]). Due to the lack of available Mxi1 isoform-specific antibodies, we cannot determine the localization of the endogenous forms by immunofluorescence at this time.

Based on the data presented in Figure 2, we believe that exogenous Mxi1-SRα, like Mxi1-SRβ, is a nuclear protein. Thus, difference in the subcellular localization cannot provide a basis for the differential effect of the two isoforms on Myc induced cellular transformation.

The evolutionarily conserved, extended proline-rich domain of Mxi1-SRα affects its suppression potential

We predicted that the basis for functional differences between Mxi1-SRα and Mxi1-

SRβ could relate to the unique amino terminal 61 amino acid (aa) extension on Mxi1-SRα (preceding its SID). As shown in Figure 3A, this extension (here named the PRD for proline-rich domain) is conserved from fish to man, and, at least in mammals, is proline and alanine rich. Hypothesizing that this PRD of Mxi1-SRα could be playing a regulatory role or encoding novel functions, we asked whether the presence of this domain is responsible for the differential effects of introduced Mxi1-SRα and Mxi1-SRβ in the REF assay. An expression construct was generated encoding a Myc-tagged version of Mxi1-SRα lacking its proline-rich domain (Fig. 3B); this construct was shown to give rise to a protein of the expected size expressed at similar levels to its full length counterpart (data not shown). When introduced with Myc+Ras in the REF assay, this construct suppressed co-transformation activity at least as well as Mxi1-SRβ (Fig. 3B, compare striped "SRαΔPRD" bar to black "SRβ" bar). Said another way, deletion of the 61 amino acid PRD from Mxi1-SRα converts Mxi1-SRα into a potent suppressor of Myc+Ras transformation. **However, the PRD does not appear sufficient on its own to convert the Mxi1-SRβ protein into a protein with α-like properties in other assays (see below).**

The extended proline-rich domain of Mxi1-SRα affects its activity on the MYC promoter

Having seen this effect of the proline-rich domain on Mxi1-SRα function at the cellular level, we next asked whether the presence or absence of this domain affects Mxi1-SRα activity on the promoters of downstream target genes. Earlier we had shown that Mxi1-SRα and Mxi1-SRβ exhibited similar effects on two synthetic reporter constructs in 293T cells [12]. Here we extended these analyses to the E-box containing promoter *ornithine decarboxylase* (*ODC*) promoter; notably this is one of the few promoters reported to be regulated by Mxi1 (and also by Myc) [16]. As shown in Figure 4A, the addition of Mxi1-SRα or Mxi1-SRβ effectors to 293T cells also carrying *ODC*-driven luciferase resulted in a

2-3-fold reduction in luciferase activity, consistent with what has been shown previously for Mxi1-SRβ on this promoter [16]. It is known that this region of the *ODC* promoter bears two E-box elements that are repressed by Mxi1 but activated by Myc (see [17] for example). As such, the similar effects of the two Mxi1 isoforms on this promoter are in the line with their similar effects on the synthetic E box reporter [12].

A second promoter shown previously to be regulated by Mxi1-SRβ is the *MYC* promoter [18,19]. For this promoter, regulation by Mxi1 has been proposed to occur not through E-box sequences but through initiator (Inr) elements and possibly also E2F binding sites present in *cis* [18,19]. **Whether the action of Mxi1-SRβ on the MYC promoter is direct or indirect remains to be elucidated.** Consistent with what has been reported previously, Mxi1-SRβ exhibited a mild, but reproducible, repressive effect on the full length human c-*MYC* promoter (Fig. 4B) [18,19]. Surprisingly, Mxi1-SRα activated this reporter (Fig. 4B). Deletion of the 61 amino acid PRD from Mxi1-SRα converted Mxi1-SRα from an activator to a potent repressor of the *MYC* promoter (Fig. 4B). **Again, whether the action of Mxi1-SRα is direct or indirect remains to be elucidate.** Of note, the same trend of Mxi1-SRβ and Mxi1-SRαΔPRD repressing, but Mxi1-SRα activating, was observed on the minimal *MYC*-P1P2 promoter (data not shown). Taken together, our findings suggest that on certain downstream target gene promoters in transient transfection experiments, Mxi1-SRα and Mxi1-SRβ exhibit distinct transcriptional effects, and these are correlated with the presence of the proline-rich domain on Mxi1-SRα.

Mxi1-SRα is able to interact with GAPDH, and these two proteins synergise to activate the myc promoter

We hypothesized that the basis for the differential effects of Mxi1-SRα and Mxi1-SRβ in several functional assays could relate to differences in their protein interaction profiles. To

address this, we established inducible HeLa cell lines expressing FLAG-Mxi1-SRα or FLAG-Mxi1-SRβ under the control of the TET ON promoter. We monitored induction as well as expression levels of the isoforms by immunoprecipitation with an anti-FLAG antibody followed by anti-FLAG Western blot analysis (Fig.5A). We then performed a FLAG pull down analysis, followed by resolution on SDS-PAGE gel and silver staining (see Fig. 5B). Several bands appearing to be present in the Mxi1-SRα but not Mxi1-SRβ lanes were **subjected to** mass spectrometry analysis (see Material and Methods). One candidate Mxi1-SRα interacting protein identified was the 38kDa GAPDH protein **which obtained a very high score with 31 matching peptides (Data not shown). This interaction was confirmed** by Western blotting analysis using the anti-GAPDH antibody [20] on the FLAG immunoprecipitates (Fig. 5C). Interestingly, this 38 kDa GAPDH protein has recently been characterized to be part of a transcriptional co-activator complex [20]. Accordingly, we next tested whether Mxi1-SRα and GAPDH could synergize to activate the *myc* promoter. Whereas GAPDH overexpression had no activating effect on the P1P2myc promoter without effector (Fig. 5D, compare lane 2 with lane 1) or even in the presence of Mxi1-SRβ (Fig. 5D, compare lane 5 and 6 with lane 1), the co-expression of GAPDH with Mxi1-SRα led to enhanced activation (Fig. 5D, compare lane 4 with lane 3). **Very interestingly, GAPDH over expression did not affect the activity of the Mxi1-SRα protein when its PRD was deleted (Fig. 5D, compare lane 7 and 8 with lane 1). Thus, all the specific properties of the full length Mxi1-SRα protein observed here appears to depend on the presence of the PRD.** Taken together, it appears that Mxi1-SRα may recruit a unique set of proteins, including GAPDH, to participate in transcriptional activation of target genes.

Discussion

In this study, we have further compared the Mxi1-SRα and Mxi1-SRβ protein isoforms that have previously been described by us to be highly similar at the levels of tissue-type expression patterns, protein interaction profiles, and transcriptional repression activity [12]. Here we extend the similarity between these isoforms by showing that, at least when exogenously introduced, both isoforms localize to the nucleus (Figure 2) and both repress the promoter of a known Mxi1 (and Myc) downstream gene target, *ODC* (Figure 4A). However, Mxi1-SRα and Mxi1-SRβ also appear to encode differential functions, and those revealed in this study relate to two distinct levels of Myc antagonism. First, contrary to Mxi1-SRβ, Mxi1-SRα is not a potent suppressor of the cellular transformation activity of Myc (Figure 1). Second, while Mxi1-SRβ has a mild, but reproducible repressive effect on the *MYC* promoter in transient expression assays, Mxi1-SRα instead activates this promoter (Figure 4B).

The finding of these differential functions is in line with the dogma that the proteome gains functional complexity by encoding multiple isoforms of a given protein, with these isoforms having shared and distinct features (reviewed in [21,22]). With respect to Mxi1-SRα and Mxi1-SRβ, this functional complexity may allow for differential regulation of Myc-dependent processes. This could occur via alterations in the balance between the two isoforms in specific cell types, developmental stages, or even during cancer pathogenesis. Regarding the latter, it is interesting to note that the Mxi1-SRα isoform (also know as Mxi1-0) was cloned initially as a gene upregulated in a neuroblastoma cell line. Moreover, in that study, the ratio between Mxi1-SRα/Mxi1-0 and Mxi1-SRβ in primary glioblastomas was shown to be increased relative to their ratio in normal brain [13]. Future studies using isoform-specific reagents could determine whether this also holds true for other cancer types,

and could ascertain whether altering the levels of Mxi1-SRα or Mxi1-SRβ can differentially impact upon cellular processes including proliferation, apoptosis, differentiation, *etc*. Isoforms of numerous proteins have been studied and compared in this manner, including alternative isoforms of members of the p53/p63/p73 (reviewed in [23]) and the Bcl2 families (reviewed in [24]).

On the molecular level, we show that the unique proline rich domain (PRD) on Mxi1-SRα contributes to the differential functions of Mxi1-SRα and Mxi1-SRβ in Myc antagonism Deletion of this domain converts Mxi1-SRα into a potent suppressor of Myc/Ras cotransformation activity (Figure 3) and also changes Mxi1-SRα's activity on the *MYC* promoter from activation to repression (Figure 4B). Relevant to this, we were intrigued by the proline-rich composition of the PRD of Mxi1-SRα, given that this is a recurring feature of transactivation domains. However, when we tested the PRD in the Gal4 heterologous reporter assay system, we did not observe it to have inherent transactivation potential ([12] and data not shown). Thus the PRD is necessary but likely not sufficient for the transactivation activity of Mxi1-SRα. Consistent with this, a chimeric protein that we generated to contain the PRD hooked up to the Mxi1-SRβ isoform (PRD-Mxi1-SRβ) is not able to activate a *myc* promoter in transient transfection experiment (data not shown**).** Thus, the activation function of **Mxi1-SRα that depends on the integrity of** the PRD appears to depend also on other **features** of the Mxi1-SRα proteins **as it cannot be simply transferred to another protein, even as closely related as Mxi1-SRβ**

We speculate that the PRD may be involved in regulating other functional domains of Mxi1 (*e.g.,* the SID or the bHLH/LZ) and/or in the recruitment of other activities. However, in some assays, the presence of this domain does not appear to distinguish Mxi1-SRα from Mxi1-SRβ (this study and [12]). This suggests that the effects of the proline-rich domain are context sensitive, and could depend on variables including cellular milieu and promoter

environment. It is of interest in this regard that, in our hands, Mxi1-SRα and Mxi1-SRβ behaved similarly on E-box containing promoters which are thought to be repressed by Mxi1 (and related Mad family members) in a basic region-, Max-, and Sin3-dependent manner (for example see [16]; also see [25]). In contrast, on the *MYC* promoter which is repressed by Mxi1-SRβ in an E-box-independent manner ([18,19]), Mxi1-SRα exerts distinct effects. It is possible that this differential regulation of target genes contributes to different biological outcomes including the effect on transformation we have observed in the REF assay (Figure 1). A very analogous scenario has been described recently for isoforms of the Wilms' tumor gene WT1. A newly identified WT1 isoform (WT1s) has been shown to arise from alternative promoter/leader exon utilization, similar to how Mxi1-SRα and Mxi1-SRβ arise. While the full length WT1 protein encodes both transcriptional repression and activation domains, WT1s lacks the repression domain and consequently has different effects on downstream targets and in growth/cancer-related assays [26].

Our Flag pull down analysis showed that Mxi1-SRα, but not Mxi1-SRβ, is able to recruit nuclear GAPDH (Figure 5B and 5C). Moreover, GAPDH seems to enhance the activating potential of Mxi1-SRα on the *myc* promoter, but has no effect on the repression effect of Mxi1-SRβ **or a Mxi1-SRα protein deleted from its PRD (Figure 5D)**. Interestingly, nuclear GAPDH/p38 has been shown previously to be recruited by Oct-1 in a co-activator complex implicated in the S phase transcription of histone H2B promoter [20]. Thus, it is tempting to speculate that Mxi1-SRα may be able to recruit co-activator complexes containing GAPDH to specific target genes resulting in activation. More and more reports suggest that GAPDH is a multifunctional protein displaying diverse activities distinct from its conventional glycolytic activity. For example, it has been shown to be able to regulate cyclin B-cdk1 activity via its interaction with the protein SET [27], to induce the pro-apoptotic mitochondrial membrane permeabilization which is essential for apoptosis [28]

or to prevent down-regulation of CSF-1 protein by binding to CSF-1 AU-rich element and thus increasing metastatic properties in ovarian cancer [29]. GAPDH is an abundant protein but its participation in many different complexes in different cellular compartment could make it limiting for some of its roles. Thus, some specific functions of GAPDH could be more sensitive than other to variation in its intracellular level or availability. Our observation that overexpression of GAPDH enhance the activity of overexpressed Mxi1-SRα indicates that it is indeed not present in sufficient amounts for Mxi1-SRα function. **In this respect, we tested if the GAPDH protein could be the limiting factor preventing the PRD alone from having a transcriptional activity by itself in the gal4 assay (data not shown) and we found that even in the presence of overexpressed GAPDH, the PRD was not sufficient to activate transcription, emphasizing the contribution of other features of the Mxi1-SRα protein.**

In the future, it would be important to uncover the full spectrum of differentially interacting proteins as well as the spectrum of downstream target genes regulated by Mxi1-SRα and/or Mxi1-SRβ, and assess the transcriptional effects of these isoforms on these targets. A better molecular grasp on these Mxi1 isoforms is necessary for understanding the precise role(s) of Mxi1 within the extended Myc network and in the context of development and cancer.

Materials and Methods

Plasmid Generation

The Myc-tagged Mxi1-SRα and Mxi1-SRβ constructs were described in [12], and the Myc and Ras expression constructs and the pvNic vector were described in [10]. The Myc tagged WR expression construct was generated by introducing the WR cDNA containing the full 5'UTR in pcDNA3.1. The coding region of Mxi1-SRα and Mxi1-SRβ were subcloned by PCR in a vector containing an amino terminal flag tag. The Mxi1-SRα ΔPRD expression construct corresponds to the full Mxi1-SRα deleted for its first 61amino acids. The *ODC* and *MYC* reporter constructs were kind gifts of Dr. John Cleveland and Dr. Linda Penn, respectively. The HA-GAPDH expression vector was obtained by amplifying GAPDH cDNA by RT-PCR on RNA from HeLa cells, followed by subcloning in an HA-tag-containing expression vector. The Tet responsive Mxi1-SRβ and -SRα expression constructs were generated by cloning the FLAG–Mxi1 fusion protein behind a tet responsive promoter. Further details of plasmids constructions are available upon request.

REF assay and foci studies

Primary REFS were prepared and transfected using calcium phosphate precipitation as described [30]. For each construct listed, 2μg was used per plate except in the "SRβ low" point where only 0.4μg of plasmid DNA was used. The number of foci obtained for each plate was counted 10-15 days after transfection. Individual foci were picked, subcloned, and expanded as described [30].

Immunofluorescence

U2OS cells were transfected with 100 ng of DNA with Fugene, and immunofluorescence was performed as described in [31] using the anti-FLAG (M2, Sigma-Aldrich, St Louis, MO, USA) or the anti-myc (Upstate, Millipore, Bedford, MA, USA) primary antibodies and the anti-rabbit coupled to FITC (Jackson Immuno Research) or the anti-mouse coupled to FITC

(Jackson Immuno Research**,** West Grove, PA, USA) secondary antibodies, respectively. Images were acquired with an Olympus BX61 epifluorescence microscope (Olympus America, Melville, NY) and a Roper Scientific CoolSNAP HQ camera (Roper Scientific, Tucson, AZ).

Transcriptional reporter assays

293T cells were transfected by the calcium phosphate precipitation method, and luciferase activity was assessed 48 hours post transfection as described in [12]. The luciferase values were normalized to protein concentration as assessed by a Bradford assay.

Protein preparation and Western blotting analysis

Protein preparation and Western blotting analysis were performed as described in [12]. In vitro transcription/translation was performed using the TNT transcription / translation system (Promega, Madison, WI, USA).

Establishment of inducible cell lines

HeLa TET ON cells (Clontech, Takara, Mountain View, CA, USA) were transfected with inducible constructs expressing FLAG-Mxi1-SRα, FLAG-Mxi1-SRβ or empty vector using Fugene. Three days after transfection, cells were selected using puromycin (1μg/mL), and on day 15 post-transfection clones were picked and expanded. After induction with doxycycline (1μg/mL), the individual clones were tested for their expression of the protein of interest.

Flag pull down / Silver Staining / Mass spectrometry Analysis

For each stable cell line, ten 15-cm-diameter plates at 80% confluence were induced with doxycycline (1μg/mL) for 24h. Immunoprecipitation was performed using the FLAG agarose antibody (Sigma #A2220) in 50mM Tris pH 7.5, 150 mM NaCl, 0.5% NP40, 5 mM EDTA and 1 mM DTT. The immunoprecipitated protein was eluted from the beads according to the Manufacter's instruction and the supernatant was run on a 12% SDS-PAGE gel. Silver staining of the gel was performed as described in [32]. Mass spectrometry was performed by

the Rockefeller University Proteomics Resource Center (New York).

Acknowledgments

The authors thank members of the Schreiber-Agus laboratory, as well as Dr. Andras Fiser, for stimulating discussions and helpful advice on the study. We thank Dr. Paul Corn for critically reading the manuscript. We thank Laina Freyer and Dr. Rachele Arrigoni for their research contributions to the project, Dr. Rob Singer for use of his microscopes, and Dr. Xavier Darzacq for his contributions with the immunofluorescence analysis. This work was supported by NCI grant 1 R01 CA92558 (NSA) **and the Association pour la Recherche contre le Cancer (ARC) (TG)**. CDD is a recipient of postdoctoral awards from the International Agency for Research on Cancer, the National Cancer Center **and from the Association pour la Recherche contre le Cancer (ARC).** Support from the Albert Einstein Cancer Center is also acknowledged.

References

[1] Lee, L.A. and Dang, C.V. (2006) Myc target transcriptomes *Curr Top Microbiol Immunol* **302**, 145-67.

[2] Cole, M.D. and Nikiforov, M.A. (2006) Transcriptional activation by the Myc oncoprotein *Curr Top Microbiol Immunol* **302**, 33-50.

[3] Kleine-Kohlbrecher, D., Adhikary, S. and Eilers, M. (2006) Mechanisms of transcriptional repression by Myc *Curr Top Microbiol Immunol* **302**, 51-62.

[4] Wade, M. and Wahl, G.M. (2006) c-Myc, genome instability, and tumorigenesis: the devil is in the details *Curr Top Microbiol Immunol* **302**, 169-203.

[5] Pelengaris, S. and Khan, M. (2003) The c-MYC oncoprotein as a treatment target in cancer and other disorders of cell growth *Expert Opin Ther Targets* **7**, 623-42.

[6] Nesbit, C.E., Tersak, J.M. and Prochownik, E.V. (1999) MYC oncogenes and human neoplastic disease *Oncogene* **18**, 3004-16.

[7] Sears, R.C. (2004) The life cycle of C-myc: from synthesis to degradation *Cell Cycle* **3**, 1133-7.

[8] Rottmann, S. and Luscher, B. (2006) The mad side of the Max network: antagonizing the function of Myc and more *Curr Top Microbiol Immunol* **302**, 63-122.

[9] Zervos, A.S., Gyuris, J. and Brent, R. (1993) Mxi1, a protein that specifically interacts with Max to bind Myc-Max recognition sites [published erratum appears in Cell 1994 Oct 21;79(2):following 388] *Cell* **72**, 223-32.

[10] Schreiber-Agus, N., Chin, L., Chen, K., Torres, R., Rao, G., Guida, P., Skoultchi, A.I. and DePinho, R.A. (1995) An amino-terminal domain of Mxi1 mediates anti-Myc oncogenic activity and interacts with a homolog of the yeast transcriptional repressor SIN3 *Cell* **80**, 777-86.

[11] Alland, L., Muhle, R., Hou, H., Jr., Potes, J., Chin, L., Schreiber-Agus, N. and DePinho, R.A. (1997) Role for N-CoR and histone deacetylase in Sin3-mediated transcriptional repression [see comments] *Nature* **387**, 49-55.

[12] Dugast-Darzacq, C., Pirity, M., Blanck, J.K., Scherl, A. and Schreiber-Agus, N. (2004) Mxi1-SRalpha: a novel Mxi1 isoform with enhanced transcriptional repression potential *Oncogene* **23**, 8887-99.

[13] Engstrom, L.D. et al. (2004) Mxi1-0, an alternatively transcribed Mxi1 isoform, is overexpressed in glioblastomas *Neoplasia* **6**, 660-73.

[14] Kawamata, N., Sugimoto, K.J., Sakajiri, S., Oshimi, K. and Koeffler, H.P. (2005) Mxi1 isoforms are expressed in hematological cell lines and normal bone marrow *Int J Oncol* **26**, 1369-75.

[15] Reinhardt, A. and Hubbard, T. (1998) Using neural networks for prediction of the subcellular location of proteins *Nucleic Acids Res* **26**, 2230-6.

[16] Wu, S., Pena, A., Korcz, A., Soprano, D.R. and Soprano, K.J. (1996) Overexpression of Mxi1 inhibits the induction of the human ornithine decarboxylase gene by the Myc/Max protein complex *Oncogene* **12**, 621-9.

[17] Pena, A., Reddy, C.D., Wu, S., Hickok, N.J., Reddy, E.P., Yumet, G., Soprano, D.R. and Soprano, K.J. (1993) Regulation of human ornithine decarboxylase expression by the c-Myc.Max protein complex *J Biol Chem* **268**, 27277-85.

[18] Lee, T.C. and Ziff, E.B. (1999) Mxi1 is a repressor of the c-Myc promoter and reverses activation by USF *J Biol Chem* **274**, 595-606.

[19] Luo, Q., Li, J., Cenkci, B. and Kretzner, L. (2004) Autorepression of c-myc requires both initiator and E2F-binding site elements and cooperation with the p107 gene

product *Oncogene* **23**, 1088-97.
[20] Zheng, L., Roeder, R.G. and Luo, Y. (2003) S phase activation of the histone H2B promoter by OCA-S, a coactivator complex that contains GAPDH as a key component *Cell* **114**, 255-66.
[21] Landry, J.R., Mager, D.L. and Wilhelm, B.T. (2003) Complex controls: the role of alternative promoters in mammalian genomes *Trends Genet* **19**, 640-8.
[22] Stamm, S., Ben-Ari, S., Rafalska, I., Tang, Y., Zhang, Z., Toiber, D., Thanaraj, T.A. and Soreq, H. (2005) Function of alternative splicing *Gene* **344**, 1-20.
[23] Murray-Zmijewski, F., Lane, D.P. and Bourdon, J.C. (2006) p53/p63/p73 isoforms: an orchestra of isoforms to harmonise cell differentiation and response to stress *Cell Death Differ*.
[24] Akgul, C., Moulding, D.A. and Edwards, S.W. (2004) Alternative splicing of Bcl-2-related genes: functional consequences and potential therapeutic applications *Cell Mol Life Sci* **61**, 2189-99.
[25] Gunes, C., Lichtsteiner, S., Vasserot, A.P. and Englert, C. (2000) Expression of the hTERT gene is regulated at the level of transcriptional initiation and repressed by Mad1 *Cancer Res* **60**, 2116-21.
[26] Hossain, A., Nixon, M., Kuo, M.T. and Saunders, G.F. (2006) N-terminally truncated WT1 protein with oncogenic properties overexpressed in leukemia *J Biol Chem*.
[27] Carujo, S., Estanyol, J.M., Ejarque, A., Agell, N., Bachs, O. and Pujol, M.J. (2006) Glyceraldehyde 3-phosphate dehydrogenase is a SET-binding protein and regulates cyclin B-cdk1 activity *Oncogene* **25**, 4033-42.
[28] Tarze, A. et al. (2006) GAPDH, a novel regulator of the pro-apoptotic mitochondrial membrane permeabilization *Oncogene* 26, 2606-20.
[29] Bonafe, N., Gilmore-Hebert, M., Folk, N.L., Azodi, M., Zhou, Y. and Chambers, S.K. (2005) Glyceraldehyde-3-phosphate dehydrogenase binds to the AU-Rich 3' untranslated region of colony-stimulating factor-1 (CSF-1) messenger RNA in human ovarian cancer cells: possible role in CSF-1 posttranscriptional regulation and tumor phenotype *Cancer Res* **65**, 3762-71.
[30] Mukherjee, B., Morgenbesser, S.D. and DePinho, R.A. (1992) Myc family oncoproteins function through a common pathway to transform normal cells in culture: cross-interference by Max and trans-acting dominant mutants *Genes Dev* **6**, 1480-92.
[31] Shav-Tal, Y., Blechman, J., Darzacq, X., Montagna, C., Dye, B.T., Patton, J.G., Singer, R.H. and Zipori, D. (2005) Dynamic sorting of nuclear components into distinct nucleolar caps during transcriptional inhibition *Mol Biol Cell* **16**, 2395-413.
[32] Blum (1987) *Electrophoresis* **8**, 93-99.
[33] Schreiber-Agus, N., Chin, L., Chen, K., Torres, R., Thomson, C.T., Sacchettini, J.C. and DePinho, R.A. (1994) Evolutionary relationships and functional conservation among vertebrate Max-associated proteins: the zebra fish homolog of Mxi1 *Oncogene* **9**, 3167-77.
[34] http://prodes.toulouse.inra.fr/multalin/multalin.html.

Titles and legends to figures

Figure 1: Contrary to Mxi1-SRβ, Mxi1-SRα is not a potent suppressor of cellular transformation by Myc and Ras.

A) (upper) Schematic representation of the different Mxi1 isoforms tested for suppressive potential in the Rat Embryo Fibroblast (REF) Transformation Assay. All of the isoforms carried Myc tags on their COOH termini. SID=Sin3 interacting domain; BR=basic region; HLH=helix-loop-helix; CT=carboxyl terminus. (lower) Western blotting analysis of *in vitro* transcription/translation reactions performed on plasmids encoding the tagged Mxi1 isoforms shown, probed with the anti-Myc tag antibody. Molecular weight is shown in kDa on the right. The sample in the first lane represents an *in vitro* transcription/translation reaction in which there was no input plasmid. Of note, a doublet is often detected in the Mxi1-SRα lane; this likely results from an alternative initiation of translation with an in-frame ATG located 78 base pair downstream of the first ATG. **B)** Graphic representation of the results obtained in the REF assay expressed as % of foci formation, with the level of foci formation obtained for the empty vector control point set to 100%. In the SRβlow point, one-fifth the usual amount of SRβ expression construct was introduced. The graph shows the results of one representative experiment out of 2 experiments performed, giving similar results. **C)** Western blotting analysis of whole cell lysates made from transformed cell lines generated from foci arising in the REF assay. E1 is from a Myc+Ras+empty vector point, α1 and α2 are from Myc+Ras+Mxi1-SRα points, and β1 and β2 are from Myc+Ras+Mxi1-SRβ points. The SRα-myc and SRβ-myc lanes represent control lysates derived from 293T cells overexpressing Mxi1-SRα-myc and Mxi1-SRβ-myc, respectively. The blot was probed with the anti-Myc tag antibody. The arrow marks the Mxi1-SRα-myc protein observable in established cell lines derived from Myc+Ras+Mxi1-SRα foci. Molecular weight is shown in kDa on the right.

Figure 2: Introduced Mxi1-SRα and Mxi1-SRβ each localize to the nucleus.

A) Schematic representation of the constructs used for the immunolocalization experiments shown in B and C. Note that the Myc-tagged isoforms carry the tag on their COOH termini, while the FLAG-tagged isoforms carry the tag on their NH2 termini. **B)** U2OS cells were transfected with the Myc-tagged constructs indicated on the left, and the introduced Mxi1 isoforms were detected by indirect immunofluorescence using the rabbit anti-Myc antibody (Upstate # 06-549) as primary antibody and anti-rabbit coupled to FITC as secondary antibody (Jackson ImmunoResearch, WestGrove, PA). **C)** U2OS cells were transfected with the FLAG-tagged constructs indicated on the left, and the introduced Mxi1 isoforms were detected by indirect immunofluorescence using the mouse anti-FLAG antibody (Sigma # F3165) as primary antibody and anti-mouse coupled to FITC as secondary antibody (Jackson ImmunoResearch, WestGrove, PA). Note that in (B) and (C), while DAPI labels all of the cell nuclei (see also phase images), only some of the cells express the introduced Mxi1 proteins, and in these the subcellular localization is nuclear. **This experiment was performed 3 times, each giving similar results.**

Figure 3: An Mxi1-SRα protein deleted for its proline-rich domain is able to potently suppress cellular transformation by Myc and Ras.

A) Alignment of the proline-rich domains of various Mxi1-SRα orthologs showing the conservation of this domain throughout evolution. The Mxi1 protein sequences were derived from the following Genbank entries: *D. rerio* (XP_709796); *C. familiaris* (XP_852395); *M. musculus* (BAE32663; also the 295 aa protein encoded by BC064453); and *H. sapiens* (NP_569157). Note that the *D. rerio* sequence is extended relative to that reported by us previously [33]. Alignments were performed using the Multalin program [34]. **B)** (top)

Schematic representation of the synthetic Mxi1-SRα ΔPRD construct (Mxi1-SRα deleted of its proline-rich domain) compared to the Mxi1-SRα construct represented as in figure 1A. (bottom) Graph of the results obtained in the REF assay expressed as % of foci formation, with the level of foci formation obtained for the Myc+Ras+empty vector control point set to 100%. The graph shows the results of one representative experiment of a total of 3 experiments performed, each giving similar results.

Figure 4: Common and distinct transcriptional effects of Mxi1-SRα and Mxi1-SRβ on downstream target gene promoters.

A) (left) Graphic representation of the results from a luciferase assay performed using the *ODC*-LUC reporter (schematic representation on top) and the Mxi1-SRβ or Mxi1-SRα effectors. Data, graphed in a log2 scale, show fold repression relative to that obtained with an empty vector effector ("empty" lane) which is set to 0. (right) Western blotting analysis using a rabbit anti-myc tag antibody to assess the expression levels of the different myc tagged effector constructs from the actual experiment graphed in (A). Molecular weight is shown in kDa on the right. **B)** (left) Graphic representation of the results from a luciferase assay performed using the *MYC*-LUC reporter (schematic representation on top) and the Mxi1-SRβ, Mxi1-SRα, or Mxi1-SRα ΔPRD effectors. Data, graphed in a log2 scale, show fold activation or repression relative to that obtained with an empty vector effector ("empty" lane) which is set to 0. (right) Western blotting analysis using a rabbit anti-myc tag antibody to assess the expression levels of the different myc tagged effector constructs from the actual experiment graphed in (B). Molecular weight is shown in kDa on the right. The experiments shown are representative examples of experiments performed at least 4 independent times, with each point done in triplicate each time.

Figure 5: Mxi1-SRα, but not Mxi1-SRβ, is able to recruit GAPDH and to synergize with GAPDH in activating the *myc* promoter.

A) anti-FLAG Western Blot (WB) of an anti-FLAG Immunoprecipitation (IP) performed on lysates from HeLa Tet ON cells expressing either empty vector, FLAG-Mxi1-SRα or FLAG-Mxi1-SRβ after 24h induction with 1μg/mL doxycycline (lanes labeled +) or without induction (lanes labeled -). Note that the induction is tightly controlled as there is no Mxi1 produced in the absence of Doxycycline. **B)** Silver staining of an anti-Flag IP performed on lysates from HeLa Tet ON cells expressing either empty vector, FLAG-Mxi1-SRα or FLAG-Mxi1-SRβ after 24h induction with 1μg/mL doxycycline. The position of the GAPDH band (specific to the Flag-Mxi1-SRα lane) that was subjected to Mass spectrometry analysis is shown with an arrow. **C)** anti-p38/GAPDH (a kind gift of Dr. Roeder) WB of an anti-FLAG IP performed on lysates from HeLa Tet ON cells expressing either empty vector, FLAG-Mxi1-SRβ or FLAG-Mxi1-SRα after 24h induction with 1μg/mL doxycycline. The GAPDH band is shown with an arrow. **D)** Graphic representation of a luciferase assay performed with the P1P2 *c-myc* promoter as the reporter construct and the HA tagged expression construct of p38/GAPDH and/or the myc tagged expression vectors of Mxi1-SRβ, Mxi1-SRα **and Mxi1-SRα deleted from its PRD**. Mxi1-SRα and Mxi1-SRβ are not regulating the P1P2 promoter as extensively as the full length myc promoter, which makes the P1P2 promoter more sensitive to the variation in GAPDH levels provided by transfection. The data show fold activation relative to empty vector. The experiment shown is a representative experiment of an experiment done **3** times where each point was done in triplicate.

Ce manuscrit a été publié dans FEBS Journal 274:4643-4653 (2007)

A

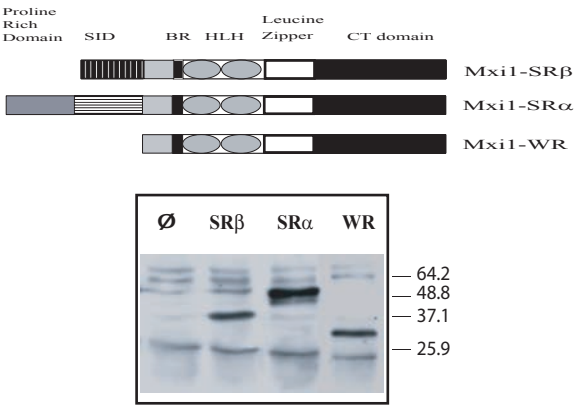

B

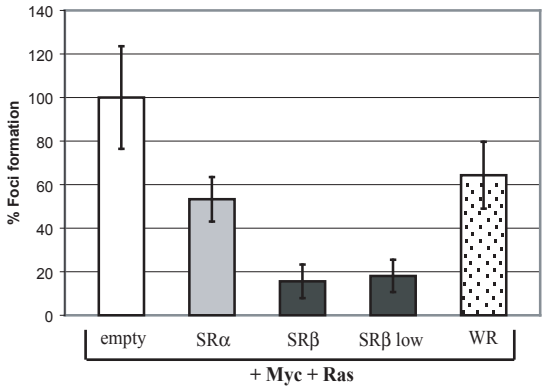

C

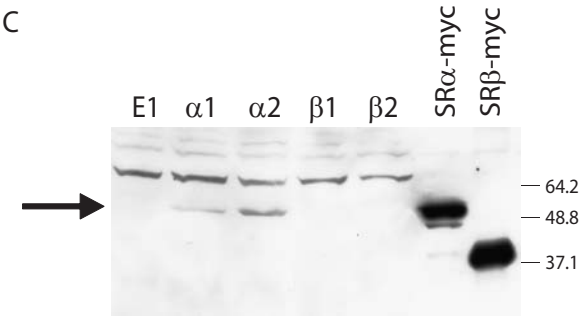

Fig 1

Ce manuscrit a été publié dans FEBS Journal 274:4643-4653 (2007)

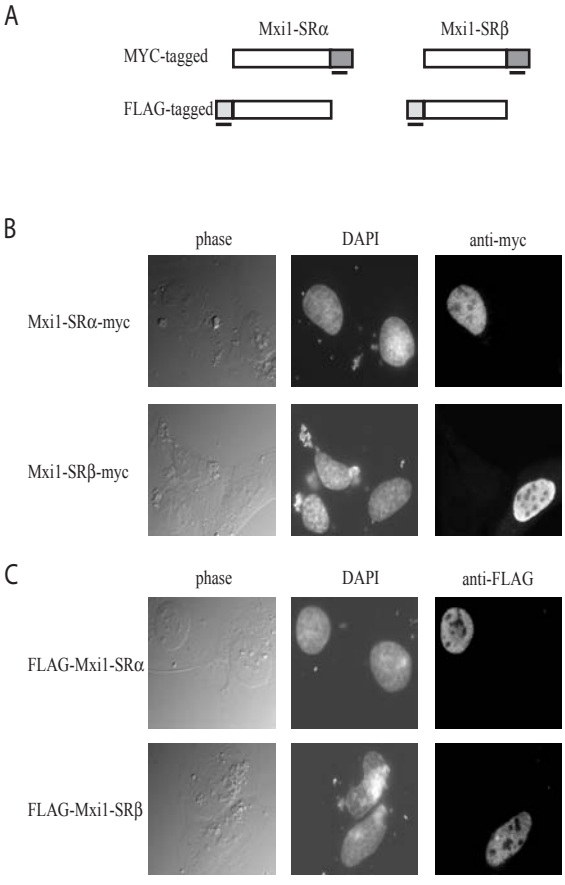

figure 2

A

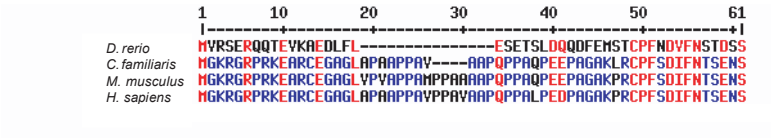
1 10 20 30 40 50 61
D. rerio MVRSERQQTEYKAEDLFL----------ESETSLDQQDFEMSTCPFNDVFNSTDSS
C. familiaris MGKRGRPRKEARCEGAGLAPAAPPAV----AAPQPPAQPEEPAGAKLRCPFSDIFNTSENS
M. musculus MGKRGRPRKEARCEGAGLVPVAPPAMPPAAAAPQPPAQPEEPAGAKPRCPFSDIFNTSENS
H. sapiens MGKRGRPRKEARCEGAGLAPAAPPAVPPAVAAPQPPALPEDPAGAKPRCPFSDIFNTSENS

B

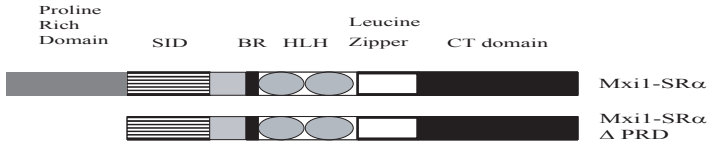
Proline Rich Domain
SID
BR
HLH
Leucine Zipper
CT domain
Mxi1-SRα
Mxi1-SRα Δ PRD

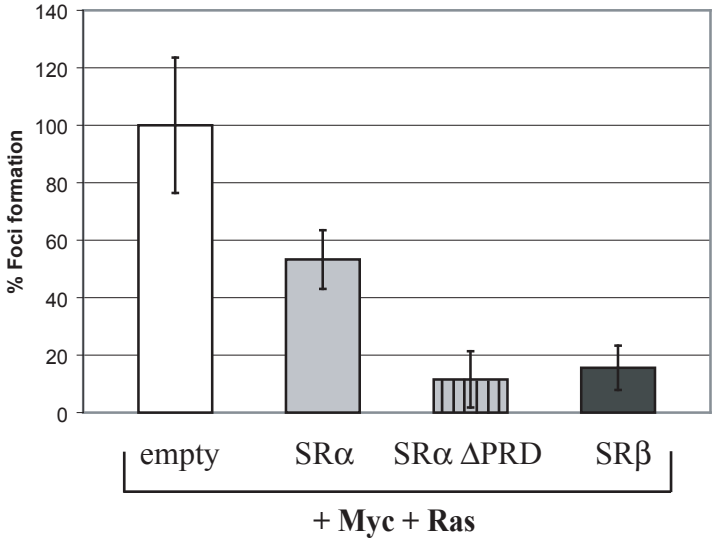
% Foci formation
140
120
100
80
60
40
20
0
empty
SRα
SRα ΔPRD
SRβ
+ Myc + Ras

Ce manuscrit a été publié dans FEBS Journal 274:4643-4653 (2007)

A

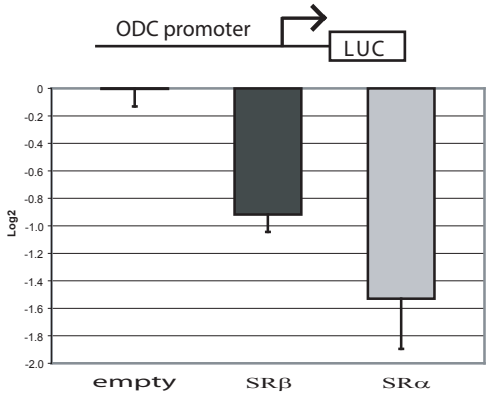

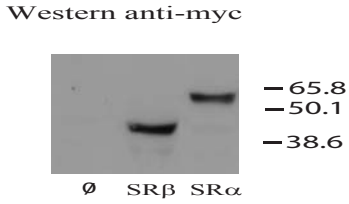

B

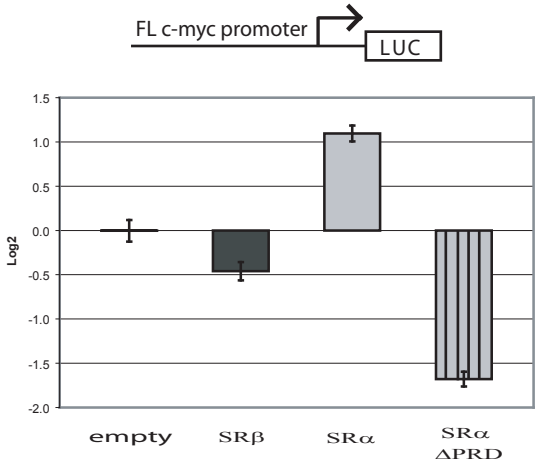

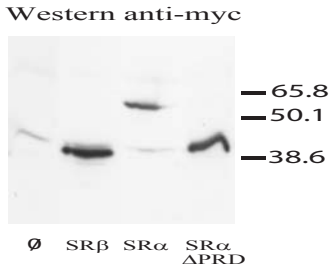

Fig 4

Ce manuscrit a été publié dans FEBS Journal 274:4643-4653 (2007)

A

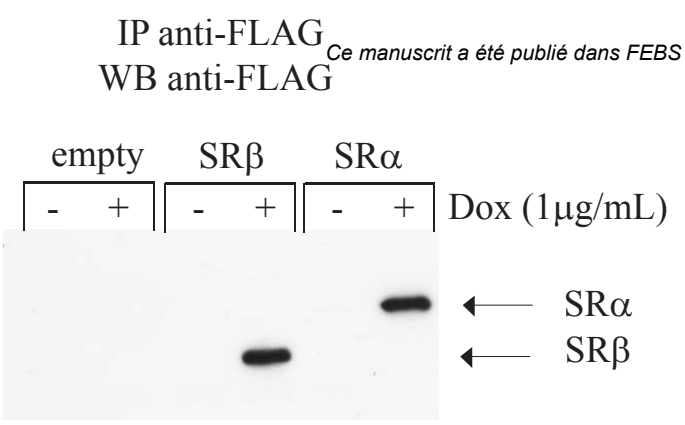

B

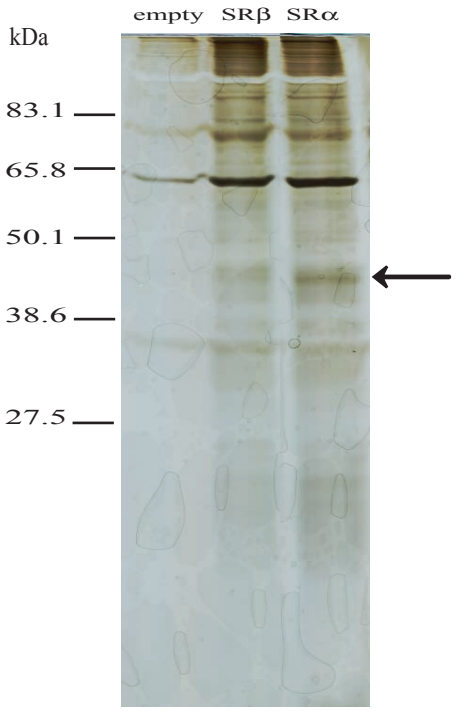

C

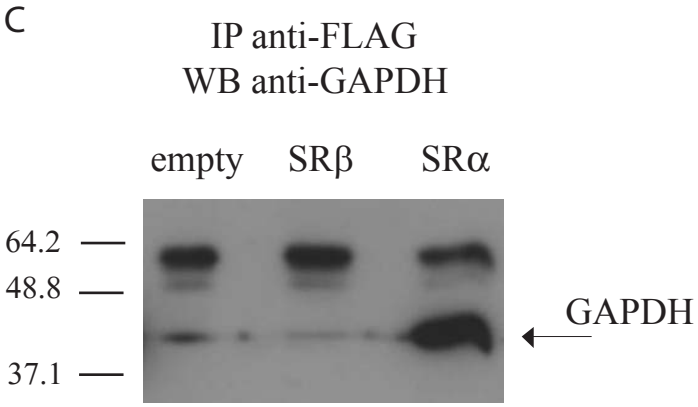

D

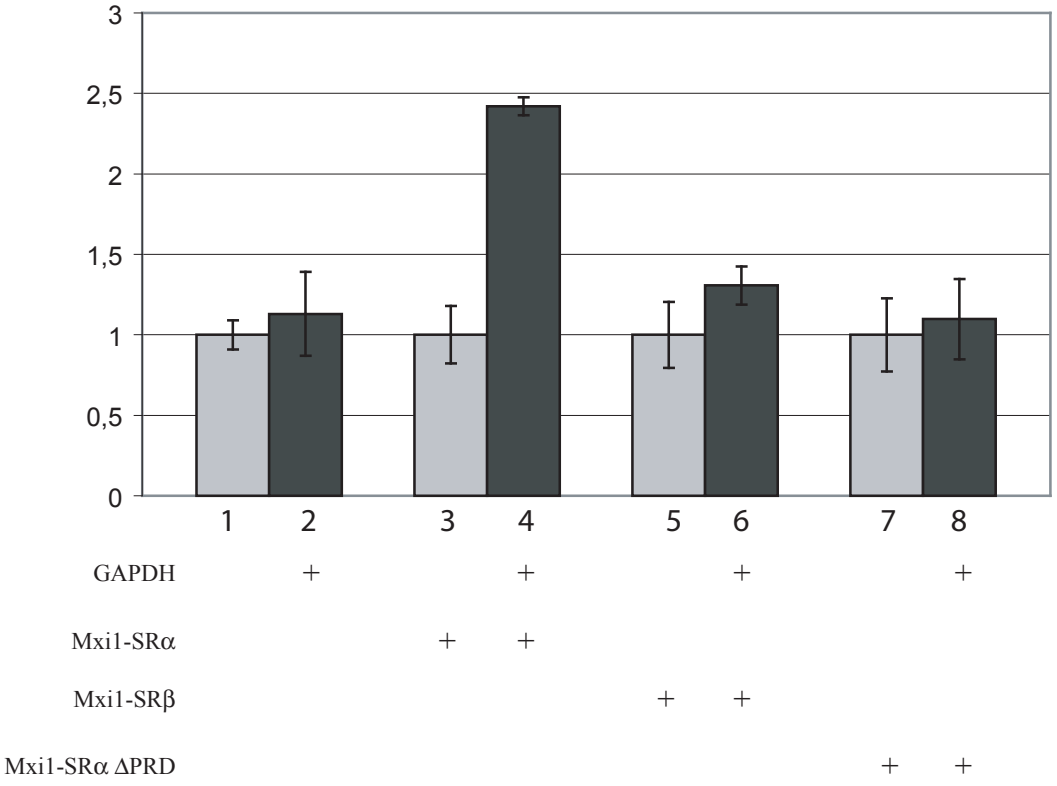

Fig 5